Engineering Failure Analysis 151 (2023) 107370

Contents lists available at ScienceDirect

Engineering Failure Analysis

journal homepage: www.elsevier.com/locate/engfailanal

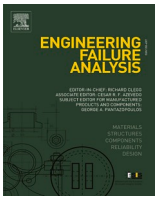

An energy-based methodology to estimate the ultimate condition of complex continuous masonry structures

C. Monteferrante [a], S. Cattari [b], A.M. D'Altri [a,c,*], G. Castellazzi [a], S. Lagormarsino [b], S. de Miranda [a]

[a] Department of Civil, Chemical, Environmental, and Materials Engineering, University of Bologna, Bologna, Italy
[b] Department of Civil, Chemical Environmental Engineering, University of Genova, Genova, Italy
[c] Department of Civil and Environmental Engineering, Princeton University, Princeton, USA

ARTICLE INFO

Keywords:
Pushover curve without softening
Masonry
Severe damage conditions
Cultural heritage structures
Bell tower

ABSTRACT

Performance-based assessment procedures for existing structures based on pushover-like nonlinear static analyses require the definition of progressive damage states on the pushover curve, which may be associated with proper limit states for safety verification purposes. In Codes, the "ultimate condition" of the structure, i.e. a damaged state in which the structure is conventionally supposed to be no longer able to carry vertical and horizontal loads, is typically identified when the base shear shows a decay higher than a given threshold (usually 15–20%). In the case of masonry structures, this issue is not always straightforward depending on the complexity of the structure and the failure mode activated. The challenge especially arises in case of monumental buildings, such as complex continuous structures (e.g. towers) and buildings composed of many macro-elements (e.g. churches), dominated by flexural failure modes (e.g. overturning mechanisms). Indeed, in these cases, pushover curves may not show a significant softening for large horizontal displacements (e.g. masonry crushing is not activated). Accordingly, the application of the aforementioned approach results impossible. In this paper, an energy-based methodology to estimate the ultimate condition of masonry structures is introduced. Although the procedure is potentially applicable to any typology of masonry structure, it is tentatively applied here to continuous tower-like structures. A preliminary calibration phase to set the energy ratio thresholds is addressed by considering various simplified benchmarks subjected to several load scenarios. To this aim, the model is subdivided into several portions, and the ratio between the dissipated energy and the total energy is tracked in each portion of the structure along with the pushover analysis. The ultimate condition of the structure is then found as soon as such ratio reaches a pre-defined threshold in a portion, calibrated in such a way to highlight where in the structure the damage is mainly localized. The methodology is then tested on a real case study application, i.e., the bell tower of the San Francesco da Paola church in Rome, modelled through a suitable nonlinear continuum modelling approach. Results prove that the methodology is general, effective, and easy to use.

* Corresponding author at: Department of Civil, Chemical, Environmental, and Materials Engineering, University of Bologna, Bologna, Italy.
E-mail address: am.daltri@unibo.it (A.M. D'Altri).

https://doi.org/10.1016/j.engfailanal.2023.107370
Received 3 February 2023; Received in revised form 5 May 2023; Accepted 29 May 2023
Available online 1 June 2023

1. Introduction

The performance-based assessment (PBA) nowadays constitutes the standard approach for seismic verification [1,2,3,4,5]. Contextually, the use of procedures based on pushover-like nonlinear static analyses is the most widespread when dealing with the structural assessment of existing structures [6]. Within this framework, a crucial issue consists of properly defining progressive damage states on the pushover curve. Indeed, once they are associated with limit states, the corresponding displacement capacities are adopted for safety verification purposes to be compared with the expected seismic demand. In particular, the definition of severe damage conditions (named "ultimate conditions" in the following), which are associated with the progressive loss of capacity of the structure to equilibrate the external horizontal actions and, even, the gravitational ones, is particularly tricky. As more deeply discussed in Section 2, this issue is usually faced by referring to conventional base shear decay thresholds, i.e., an approach that presupposes a softening phase of the pushover curve. Whatever the approach adopted, the definition of the displacement capacity associated to the ultimate damage/performance state appears essential, since in most of the verification procedures, as those based on the N2 method [7] (like [1]), it remarkably influences the resulting bilinear equivalent curve, i.e. the main input of the verification procedure.

Following this approach, the PBA becomes even more challenging when dealing with complex unreinforced masonry (URM) structures, especially in the case of monumental buildings (like palaces, churches, fortresses, towers, …) given their irregular geometries and the highly nonlinear mechanical response of masonry. A comprehensive classification of monumental buildings as a function of their expected behavior in seismic-prone areas is provided in [8], while an overview of how the displacement-based approach may be practically customized to various architectural configurations is illustrated in [9], as resulting from the PERPETUATE FP7 European research project. Some examples of applications of PBA to various monumental buildings are presented in [10,11,12,13,14].

As for the ability of models of describing the nonlinear behavior of masonry concerns, various modelling approaches are available in the literature, as classified and critically reviewed in [15], distinguishing among block-based models (BBM), (ii) continuum models (CM), (iii) equivalent frame models (EFM), and (iv) geometry-based models (GBM). Moreover, in [16] a critical review of the current use and open issues on nonlinear modelling of URM structures has been illustrated. Currently, in the case of monumental URM buildings, continuum models appear the most promising and efficient modelling strategy, given their capability to deal with complex architectural configurations with a feasible computational demand and to overcome some limitations of other approaches (such as, in comparison with EFM, the need of defining a priori the portion which the nonlinear behavior has to be concentrated to and the possibility of accounting in an integrated way for the in-plane and out-of-plane response).

In CM, masonry is modelled as a homogeneous continuum, without distinction between blocks and mortar layers. Even though the computational effort is lower than other modelling strategies, the formulation of suitable constitutive laws for masonry, and hence the definition of the mechanical properties, is challenging. Orthotropic nonlinear continuum constitutive laws represent optimal solutions, but their application is limited due to computational effort and the large number of material properties required. Examples of this approach have been proposed in [17,18,19,20,21,22]. Another simplified and efficient approach for continuum models is based on isotropic nonlinear constitutive laws. Several smeared crack, damage and plastic-damage models have been utilized for masonry structures, although they cannot account for the anisotropic nature of masonry. Particularly for historic monumental buildings, this approach represents a good compromise, given the presence of multi-leaf irregular randomly-assembled masonry (and so the anisotropic nature of masonry response is less evident), and the need of few mechanical properties (as destructive testing needs typically to be strongly limited or is even forbidden for preservation reasons). Indeed, many applications of 3D isotropic nonlinear continuum models to historic towers [23,24,25,26,27,28] and churches [29,30,31] can be found in the literature.

Although the significant advances in numerical modelling [32,33], the definition of the severe damage conditions on the pushover curve, however, still poses some significant issues. In particular, this paper deals with the cases which do not show significant base shear decays for large horizontal displacements, leading to a non-trivial identification of the ultimate condition of the structure based on the current heuristic criteria proposed in Codes, as discussed in Section 2.

The challenge especially arises in complex continuous structures (e.g., towers) and buildings composed of many macro-elements (e.g. churches), dominated by flexural failure modes which are not associated to a significant degradation of the strength capacity.

In this context, some preliminary advances to identify ultimate conditions have been developed within the framework of nonlinear dynamic analyses. For example, it is worth mentioning the work in [34], where a hierarchy of dissipated energy to give a scale of the vulnerability of the macro-elements that compose a church has been investigated. Additionally, the energy dissipated in different portions of historical masonry bell towers subjected to spectrum-compatible artificial and real accelerograms have been investigated in [35].

In this paper, an energy-based methodology is introduced to estimate a severe damage state, ascribable to the ultimate condition defined in many Codes [1,2,3,4]. Although the procedure is potentially applicable to any typology of cultural heritage structure, the approach is tentatively applied to continuous tower-like structures by performing nonlinear static analyses.

The paper is structured as follows. Additional motivations of this research are given in Section 2. The core aspects of the energy-based methodology are highlighted in Section 3. Section 4 presents and discusses the pre-analyses for tower-like large-scale masonry structures. This leads to a preliminary calibration for setting the energy ratio thresholds to be assumed. To this aim, various simplified benchmarks subjected to several load scenarios, and modelled through a suitable nonlinear continuum modelling approach, are considered. According to the proposed approach, the model is subdivided into several portions, and the ratio between the dissipated energy and the total energy is tracked in each portion of the structure along with the pushover analysis. The application of the methodology to a real case study, consisting of the bell tower of the San Francesco da Paola Church in Rome modelled through a plastic-damage continuum modelling approach, is shown and discussed in Section 5. Finally, Section 6 collects the main conclusions of

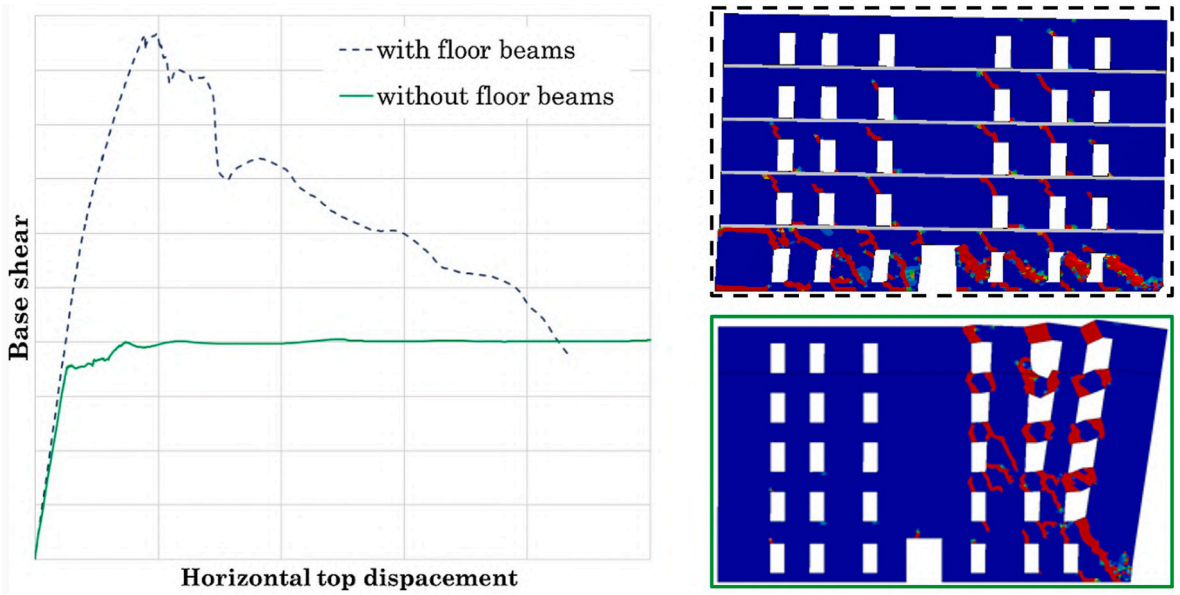

Fig. 1. Example of a masonry structure that shows softening behavior when concrete floor beams are present, while no softening is observed without concrete floor beams (adapted from [16,48]).

this work.

2. Motivations

The definition of the ultimate condition of URM structures is treated in current Codes by adopting various approaches. As usually assumed in Codes, the "ultimate condition" is herein considered as the Collapse Prevention Limit State. [2] proposes to check the attainment of given damage levels in each single elements by considering drift thresholds set at pier scale. [1] and [3] refer to heuristic criteria based exclusively on the strength degradation rule, which identifies the ultimate condition as soon as the base shear shows a given decay (usually equal to 20% in the case of URM buildings). [4] provides further recommendations to [3] for URM buildings characterized by stiff or flexible diaphragms or with irregular configurations such to promote torsional effects. In particular, such integrations propose to combine the pure heuristic criteria with checks addressed to detect the concentration of the damage on single walls or a single story. More recently, a multiscale approach that integrates checks to monitor the spread of the damage along the building by considering panels and macro-elements (where the macro-element is intended as an assemblage of components, like vertical walls or diaphragms) has been proposed in [36]. This approach may be consistently applied for interpreting both real evidence and numerical simulations, and is in line with what previously proposed in [37] and [9], and partially received by [4]. Other works recommend the use of combined criteria, see e.g. [38]. In the recent experience made within the RINTC project [39,40], according to [41,42], the attainment of the Global Collapse (GC) condition corresponds to a degradation of the total base shear below 50% of the maximum base shear. To detect this condition, the Engineering Demand Parameter (EDP) monitored during the analysis has been identified as the maximum inter-story drift (accounting also for the contribution of rotations) among all walls and stories in the direction of analysis. For each direction, the minimum values among all the analyses were then assumed as GC performance state thresholds.

However, the application of the aforementioned rules is often tricky, and in some cases even not applicable, as debated in the following.

On the one hand, EFM [43,44,45,46] directly implement the drift thresholds recommended in Codes to monitor the attainment of the collapse condition at the scale of single elements, i.e. piers and spandrels, which are identified a priori. Once a pier overcome this drift limit, its capability to equilibrate horizontal actions becomes null and, consequently, the overall base shear shows a drop. Accordingly, the ultimate condition of the structure is easily and always trackable in EFM.

On the other hand, CM simulate the masonry quasi-brittle behavior at the material scale. Accordingly, a significant softening cannot always be observed. Indeed, this depends on the loading conditions and failure mechanisms. Although drift checks analogous to those in EFM may be applied [47], they would introduce further challenging issues (e.g., distinction between flexural and shear failure modes).

Moreover, the identification of structural elements (piers and spandrels) in monumental buildings is typically impractical due to complex and irregular geometries. Consequently, the application of criteria based on drift checks or interstory thresholds is generally infeasible. Typical examples consist of continuous structures like towers, churches, or configurations in which the failure modes cannot be properly interpreted according to a pier-spandrel scheme. The case of churches is emblematic as they are composed of various

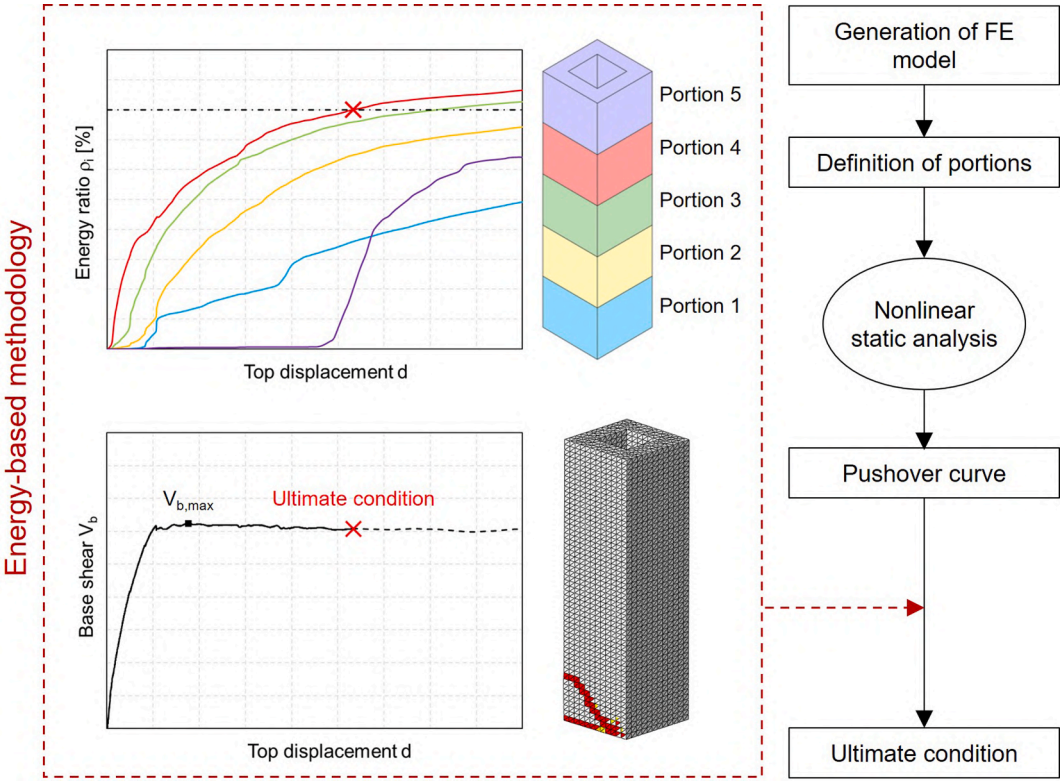

Fig. 2. Procedure to identify the ultimate condition of the structure using the energy-based methodology.

interacting portions. Indeed, the pushover curve may not present a significant softening even though some macro-elements show severe damage. The real case study investigated in Section 5 clarifies this situation.

Another clarifying example is shown in Fig. 1, where the pushover curves of an in-plane loaded masonry façade are shown together with the crack pattern. In particular, two analyses are conducted: (a) the first one with concrete floor beams, which shows a significant softening after the diagonal shear failure of the masonry walls at the ground level, (b) the second case without concrete floor beams, which is associated with a plateau in the pushover curve and no softening response is highlighted. Indeed, case (b) is ascribable to the activation of an overturning mechanism of a portion of the façade. Such plateau would proceed up until crushing failure is triggered in the bottom right corner, which would cause softening in the pushover curve. However, crushing failure may not arise, e.g., if the vertical loads are not sufficient to generate compressive failure.

It should be stressed, therefore, that the same structure would show different ultimate displacements and different tendency to softening depending on the failure mode, which is influenced by the vertical load, boundary conditions, material strengths, horizontal load distribution, opening locations, etc.

All these issues highlight the need for a more flexible approach able to effectively support the interpretation of results with the aim of easily detecting the concentration of damage in portions of the structure despite the overall trend of the global pushover curve. Of course, such an approach becomes particularly useful when the strength degradation rule cannot be used and, generally, it cannot be known a priori if the structural response will eventually show softening in the pushover curve. With this in mind, an alternative to the strength degradation rule is presented in the following.

3. Energy-based methodology

Here, an energy-based methodology is introduced to estimate the ultimate condition of the structure. In particular, the trend of the ratio between the dissipated energy and the total energy in each portion of the structure is monitored and used to define the ultimate condition of the structure on the pushover curve.

The flowchart of the proposed procedure is shown in Fig. 2. Once defined a suitable numerical model of the whole building, the structure is divided into various portions. These portions may be identified according to geometrical, material and architectural features. Indeed, reference should be made to the construction phases, taking into account, e.g., additions, discontinuity between portions, etc. In addition, also architectural elements (macro-elements) should be considered, e.g., triumph arch, apse, etc.

Nonlinear static analyses are performed through the application of the gravitational loads, as well as a system of horizontal forces to push the structure. Accordingly, the evolution of the horizontal displacement of a control node on the top of the structure is tracked together with the base shear.

For each i-th portion of the structure, the ratio ρ_i between dissipated energy and total energy is evaluated as:

$$\rho_i = E_i^{diss}/E_i^{tot}.$$

In the framework of modelling through continuum models with nonlinear plastic constitutive laws, the plastic dissipated energy in the i-th portion of the structure can be expresses as:

$$E_i^{diss} = \int_{V_i} \boldsymbol{\sigma}^T \boldsymbol{\varepsilon}^{\boldsymbol{pl}} dV,$$

where $\boldsymbol{\sigma}$ is the stress vector, $\boldsymbol{\varepsilon}^{\boldsymbol{pl}}$ is the plastic strain vector, V_i is the volume of the i-th portion. The total energy in the i-th portion of the structure is defined as:

$$E_i^{tot} = \int_{V_i} \boldsymbol{\sigma}^T \boldsymbol{\varepsilon} dV,$$

where the total strain vector $\boldsymbol{\varepsilon}$ is calculated as $\boldsymbol{\varepsilon} = \boldsymbol{\varepsilon}^{\boldsymbol{el}} + \boldsymbol{\varepsilon}^{\boldsymbol{pl}}$, with $\boldsymbol{\varepsilon}^{\boldsymbol{el}}$ the elastic strain vector.

When ρ_i reaches considerable values (e.g., beyond 50%) it indicates a high dissipation of energy and, hence, a high excursion in the nonlinear field in the i-th portion of the structure. Therefore, it suggests a condition in which the damage pattern may be widespread, and so it can be used to investigate the structural ultimate condition.

A suitable way to track the results could be through the graph $d-\rho_i$, where d is the top horizontal displacement of the structure. Various curves will be then representative of the behavior of each i-th portion as a function of the control point displacement. Additionally, it may appear convenient to define, for each value of the top horizontal displacement d, the maximum value of the ratio between dissipated energy and total energy ρ_{max}:

$$\rho_{max} = \max(\rho_i).$$

When this ratio reaches a pre-defined threshold, it identifies the ultimate condition of the structure. The reference threshold is established through specific pre-analyses, as those exemplified in Section 4. This may be then reported on the pushover curve $d-V_b$, where V_b is the base shear, so that to define the ultimate condition in the pushover curve. Together with the dissipated energy, a fundamental aspect to take into account is obviously the damage pattern, which provides information about the nature of the considered failure mode.

As already anticipated in Section 2, when dealing with real complex structures, their subdivision into portions could be non-trivial. Indeed, the macro-elements of the structure may interact with each other, and irreversible deformations may occur at the interface between different macro-elements. In these cases, a preliminary identification of the critical zones can be conducted [49], also through abacuses of damage mechanisms (as discussed for churches in [10] and for fortresses in [50,51]). Alternatively, it is possible to apply the procedure proposed in [52] which firstly requires the execution of a modal analysis on the 3D finite element model of the whole structure to define the load patterns proportional to the vibrational modes to be applied on each unit. In this case, in fact, it can be reduced to sub-structures with simpler behaviors and each pushover produces a concentration of damage in the macro-element itself.

4. Pre-analyses

In the following, various simplified geometries are investigated with the aim of establishing the reference threshold representative of their ultimate condition. Particularly, the geometries considered are ascribable to macro-elements which may present a configuration either isolated or inserted in a more complex structure. To describe the non-linear material behavior, the isotropic plastic-damage model developed in [53] was adopted with the various parameters appropriately calibrated, as described in Section 4.1.1. Then, a comparison of the different benchmarks is conducted to explore the thresholds of energy dissipated by the different systems, using also the evaluation of damage contour plots.

4.1. Numerical modelling

4.1.1. Constitutive model

In this research, the continuum plastic-damage material behavior based on the isotropic model proposed by Lee and Fenves [53] is adopted for masonry. Tensile and compressive responses are ruled by two independent damage variables (tensile $0 \le d_t < 1$, and compressive damage $0 \le d_c < 1$). Accordingly, the uniaxial stress–strain relationships can be represented by:

$$\sigma_t = (1-d_t)E_0\left(\varepsilon_t - \varepsilon_t^{pl}\right)$$

$$\sigma_c = (1-d_c)E_0\left(\varepsilon_c - \varepsilon_c^{pl}\right)$$

where E_0 is the initial elastic modulus, d_t and d_c the scalar damage variables, ε_t and ε_c are the total tensile and compressive strains, and ε_t^{pl} and ε_c^{pl} are the plastic tensile and compressive strains. It should be herein pointed out that, generally, masonry shows an anisotropic mechanical behavior. Nonetheless, the mechanical analysis of anisotropic media can be cumbersome due to the large number of properties that need to be defined. Although this feature may have a remarkable effect in small masonry walls, it is expected to be less

Table 1
Uniaxial behavior and damage evolution for compressive and tensile responses.

	Stress [MPa]	Inelastic strain [-]	Damage parameter [-]
Compressive behavior	4.80	0	0
	4.80	0.002	0
	0.60	0.009	0.9
Tensile behavior	0.11	0	0
	0.01	0.001	0.9

Table 2
Mechanical parameters adopted for masonry.

Young's modulus	Poisson's ratio	Density	ψ	ε	f_{b0}/f_{c0}	K_c	VP
1440 MPa	0.2	1800 kg/m^3	10°	0.1	1.16	0.667	0.0001

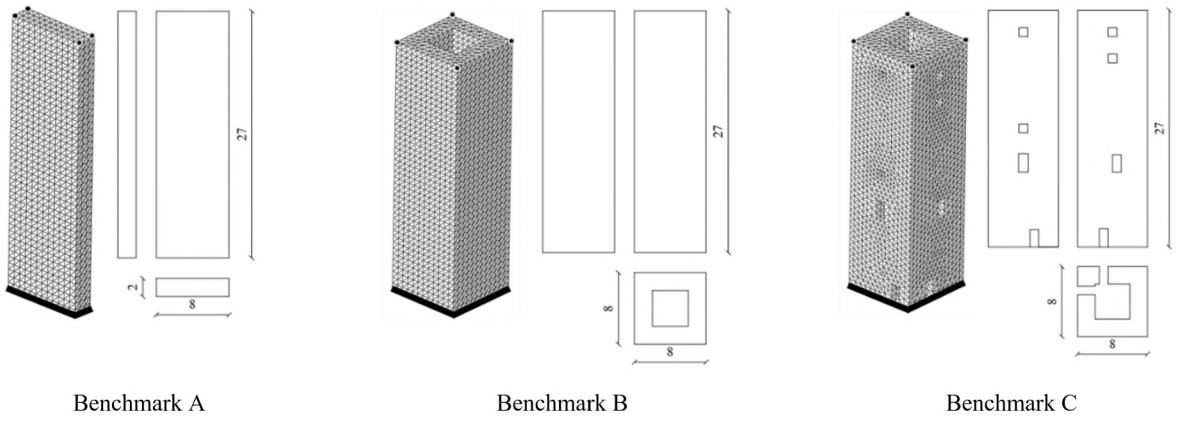

Fig. 3. Geometric features of the benchmarks considered.

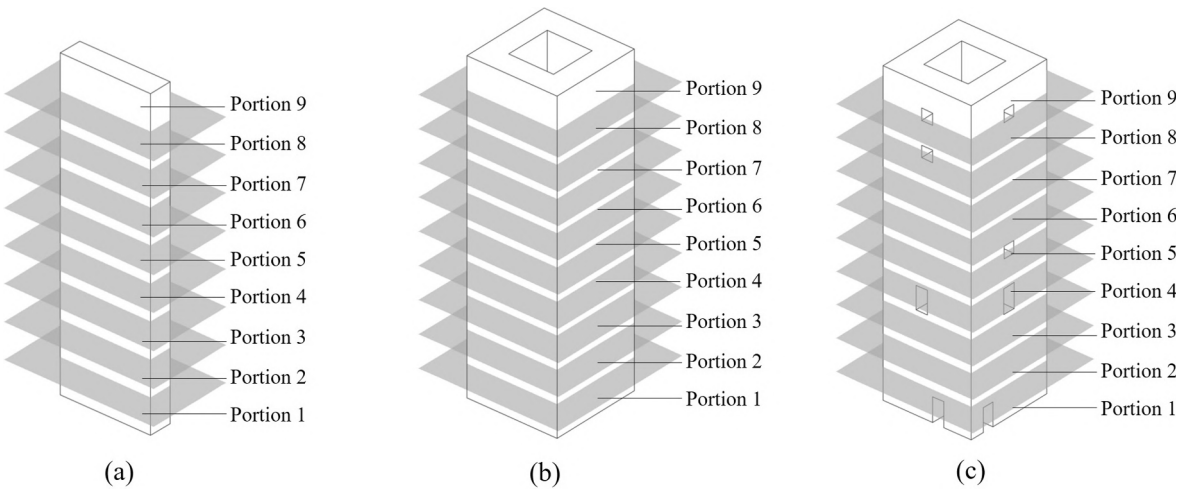

Fig. 4. Definition of portions (3*m* case) for (a) Benchmark A, (b) Benchmark B, and (c) Benchmark C.

significant at the large-scale level of historic masonry structures, characterized by multi-leaf thick walls. Finally, the constitutive model here adopted has been widely validated for masonry, e.g., by means of the comparison with other modelling approaches (e.g., in [54,55]), highlighting its capability to account for both flexural and shear wall collapse mechanisms.

Table 1 collects the parameters adopted to model the compressive and tensile behavior of the masonry, in agreement with available material data [4,30] as representative of a typical historic masonry material.

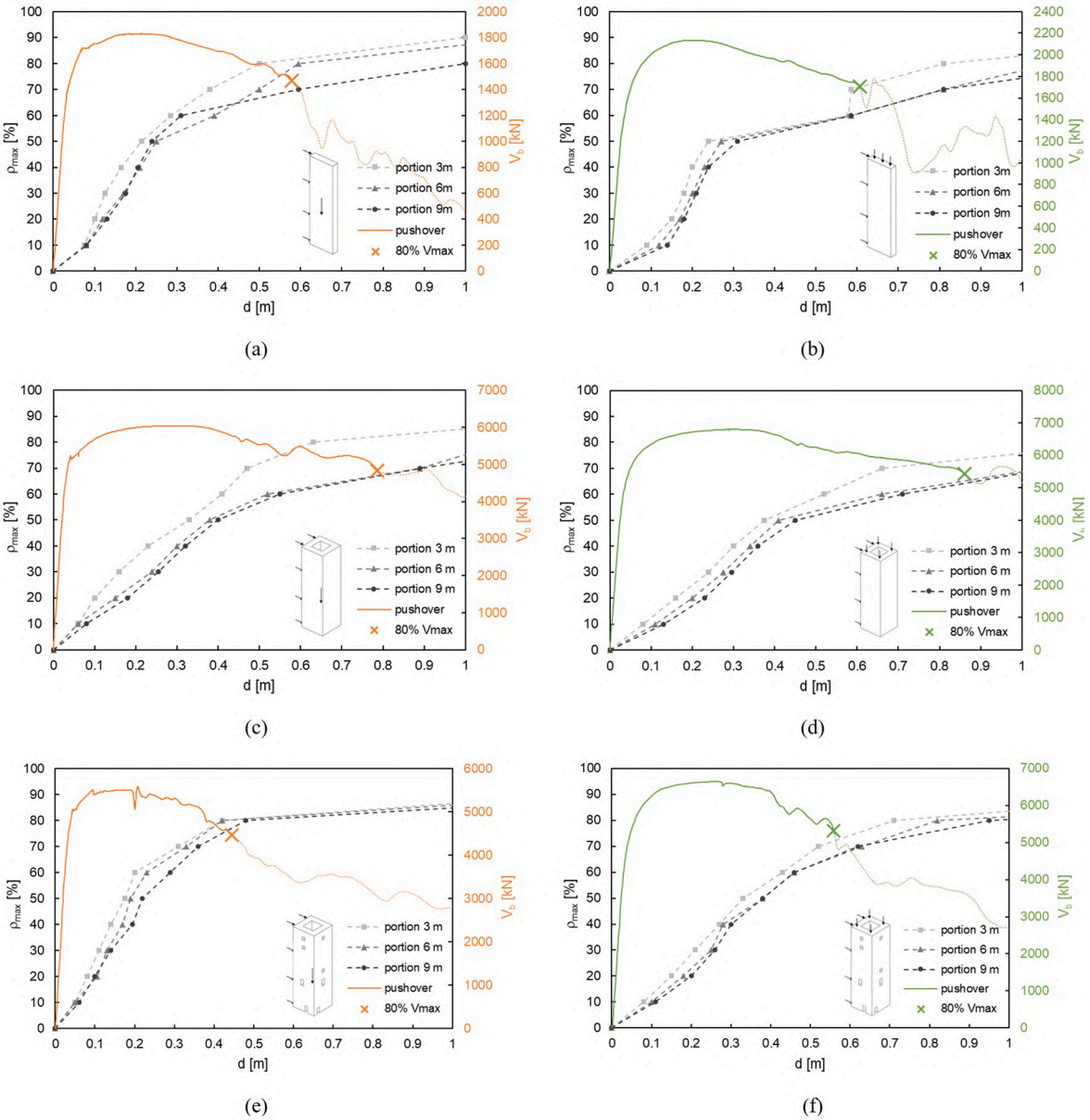

Fig. 5. Pushover curves and energy ratio ρ_{max} evolution of the three benchmarks, considering different load scenarios and subdivisions: (a) Benchmark A – GR, (b) Benchmark A – PR, (c) Benchmark B – GR, (d) Benchmark B – PR, (e) Benchmark C – GR, (f) Benchmark C – PR.

Such model is based on a Drucker-Prager yield surface. The plastic potential is characterized by the dilatancy angle ψ, and by a smoothing parameter ϵ. The yield surface is specified by the ratio between the biaxial f_{b0} and uniaxial f_{c0} initial compressive strengths and a constant K_c, which represents the ratio of the second stress invariant on the tensile meridian to that on the compressive meridian at initial yield. Besides, the viscosity parameter *VP* prevents convergence issues, allowing stresses to locally slightly exceed the yield. The values of all the above parameters are reported in Table 2, in agreement with reference works [30,33,25].

4.1.2. Numerical set-ups and load scenarios

The analyses are carried out on three different structural benchmarks (Fig. 3), which can be seen as simplifications of a masonry tower: (a) Benchmark A – wall panel, (b) Benchmark B – tower-like structure with no openings, (c) Benchmark C – tower-like structure with openings. The layout of openings adopted in the case C are inspired by the reals case study then investigated in Section 5.

A two-step analysis approach is implemented. In the first step, vertical loads are applied and two options are considered:

- *gravity* (GR): the structure is loaded vertically only by the gravitational load;

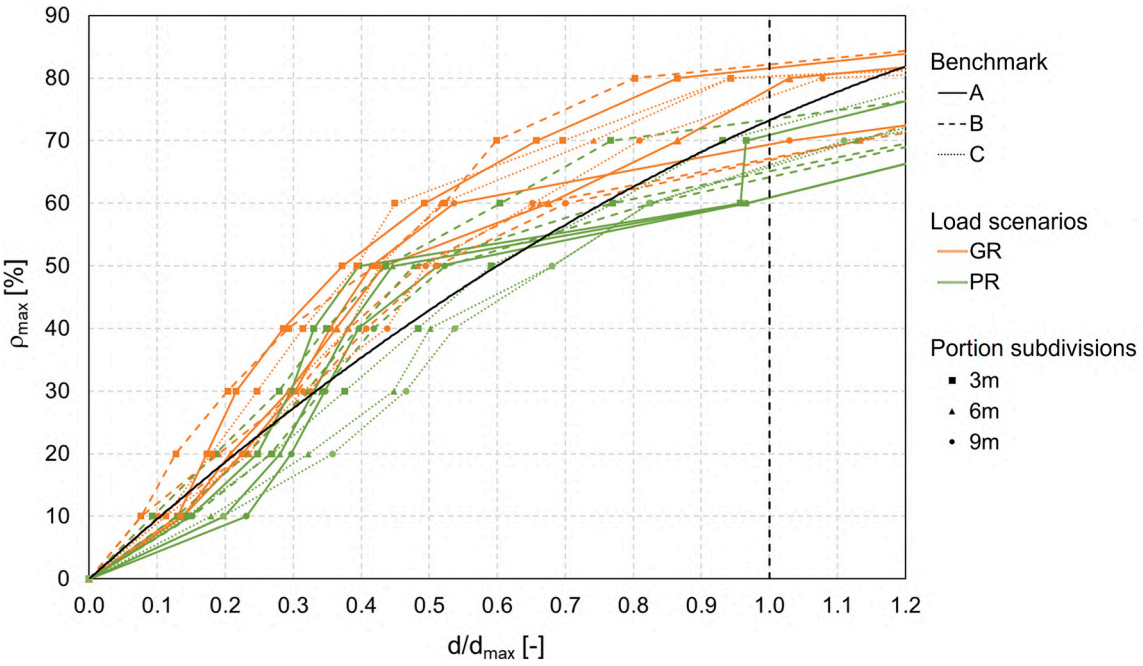

Fig. 6. Evolution of ρ_{max} along with a nondimensional measurement of the top displacement d/d_{max}.

- *pressure 10%* (PR): the structure is loaded vertically so that to induce an axial load ratio (ALR), the ratio between the vertical stress and the compressive strength of masonry, equal to 10%, i.e., an ALR which may be reasonably found in existing masonry structures [56].

In the second step, horizontal mass proportional loads are applied and the evolution of the displacement of a control node at the top of the structure is tracked together with the base shear. A quasi-static direct-integration implicit dynamic algorithm, which has been found more robust than arc length methods [25], has been adopted.

The three benchmarks are subdivided into horizontal portions of different heights, 3*m*, 6*m* and 9*m* (see an example in Fig. 4 for the 3*m* case), to assess the influence of layer size on the output. Solid 4-node tetrahedral finite elements with linear shape functions having an average mesh size equal to 0.65*m* were used in the discretization of the models. In particular, 10,113 elements for Benchmark A, 36,390 for Benchmark B, and 38,235 for Benchmark C are considered.

It should be here highlighted that a simplified seismic assessment of isolated masonry towers, that can be seen as cantilever structures undergoing global flexural failure mechanisms, could be based on the so-called behavior factor [10]. Although significant advancements have been lately developed on the behavior factor of masonry towers [57], reference behavior factors are not herein considered. Indeed, the benchmarks in Fig. 4 (that are used to calibrate the energy ratio threshold) account for the specific structural features of the real case study application (Section 5), e.g., in terms of overall dimensions, material properties, slenderness, vertical loads, and opening locations (Benchmark C only). Accordingly, this calibration appears more accurate than using more conventional behavior factors. Finally, it should be here highlighted that all the cases considered (18 in total) show softening in the pushover curve, allowing for a consistent calibration of the energy ratio threshold.

4.2. Numerical results

A total of six pushover analyses are carried out. Particularly, two scenarios (GR and PR) are considered for each benchmark, and three different subdivisions into portions are considered for each analysis. The pushover curves obtained for each case are reported in Fig. 5. Particularly, the top horizontal displacement *d* has been computed as the average of the horizontal displacements of the 4 top-corner nodes of the structure. As it can be noted in the pushover curves, they typically show softening. In particular, the point corresponding to a 20% shear decay is marked with a cross and it is assumed as reference to define the ultimate condition of the benchmarks.

For each case, the evolution of the maximum energy ratio ρ_{max} is tracked in the $d-\rho_{max}$ plane (Fig. 5). For simplicity, the curves in the $d-\rho_{max}$ plane are shown by means of discretized energy levels (10%, 20%, …, 100%). In other words, the $d-\rho_{max}$ curves show the evolution of the energy ratio along with the pushover analysis. It is worth noting that similar trends are observed for the 3 *m*, 6*m* and 9*m* subdivisions, although slightly higher for the 3*m* case. Therefore, the choice of subdivision does not appear to considerably influence the trend of the $d-\rho_{max}$ curves.

Fig. 6 shows for each case the evolution of ρ_{max} along with a nondimensional measurement of the top displacement d/d_{max}, where

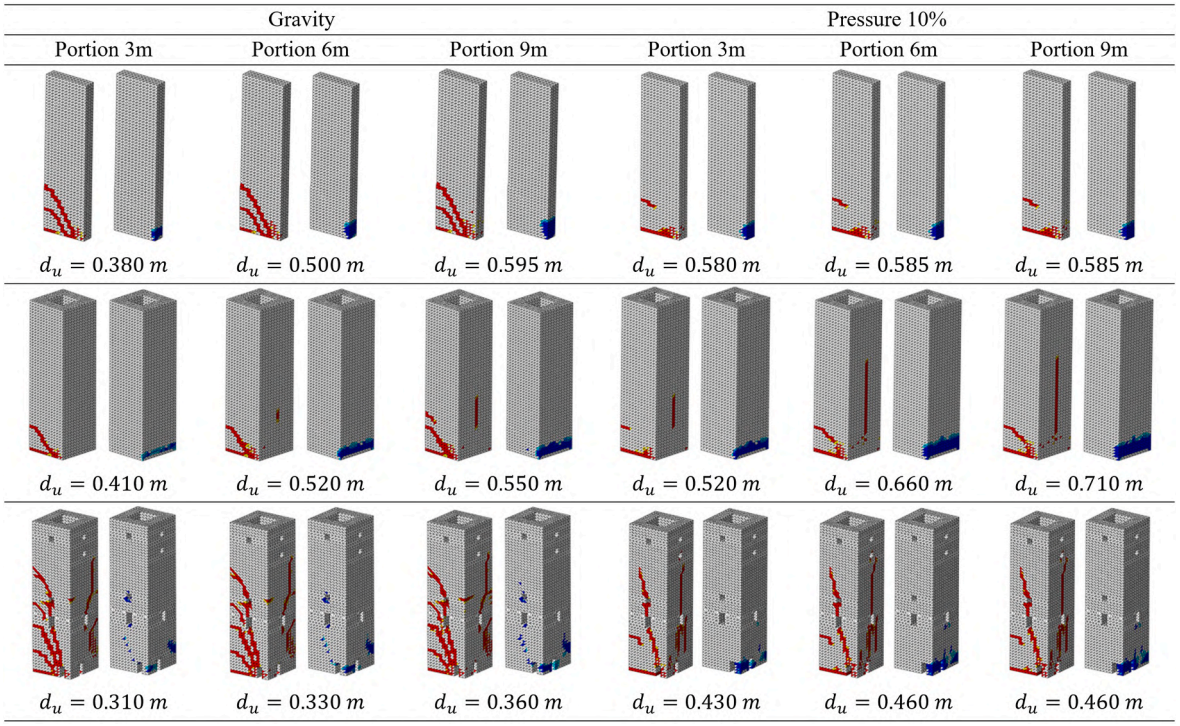

Fig. 7. Tensile (left, red color) and compressive (right, blue color) damage contour plots of the benchmarks corresponding to $\rho_{max} = 70\%$. (For interpretation of the references to color in this figure legend, the reader is referred to the web version of this article.)

Fig. 8. San Francesco da Paola church: (a) church view, (b) bell tower view, (c) plan.

d_{max} is the displacement corresponding to a 20% base shear decay. As it can be seen, the normalized curves show a rather consistent trend, and they reach $d/d_{max} = 1$ with a ρ included between 60% and 80%. If a parabolic trend line is coarsely used to fit the various curves (black curve in Fig. 6), such trend line reaches $d/d_{max} = 1$ with a value of ρ very close to 70%. Then, this value of ρ (70%) may be seen as a threshold to be used within the energy-based methodology for similar tower-like structures with akin mechanical properties, i.e., a pre-defined threshold.

Fig. 7 shows the damage contour plots corresponding to the achievement of $\rho_{max} = 70\%$ for the analyses considered in Fig. 5. As it can be noted, they clearly show the zones which reached the full degradation (in tension and in compression) of the material in the structure. Tensile cracks typically develop in a diagonal pattern, with different inclinations between the considered cases, while compressive damage always show the development of crushing in the compressed toe. By inspecting the damage contour plots at $\rho_{max} = 70\%$, it emerges that the crack patterns effectively provide an indication that the ultimate condition of the structure has been reached for all the benchmarks considered. Particularly the stopping condition at the above-mentioned energy ratio results in realistic and similar damage patterns for the different cases, independently on the scheme of subdivision in portions.

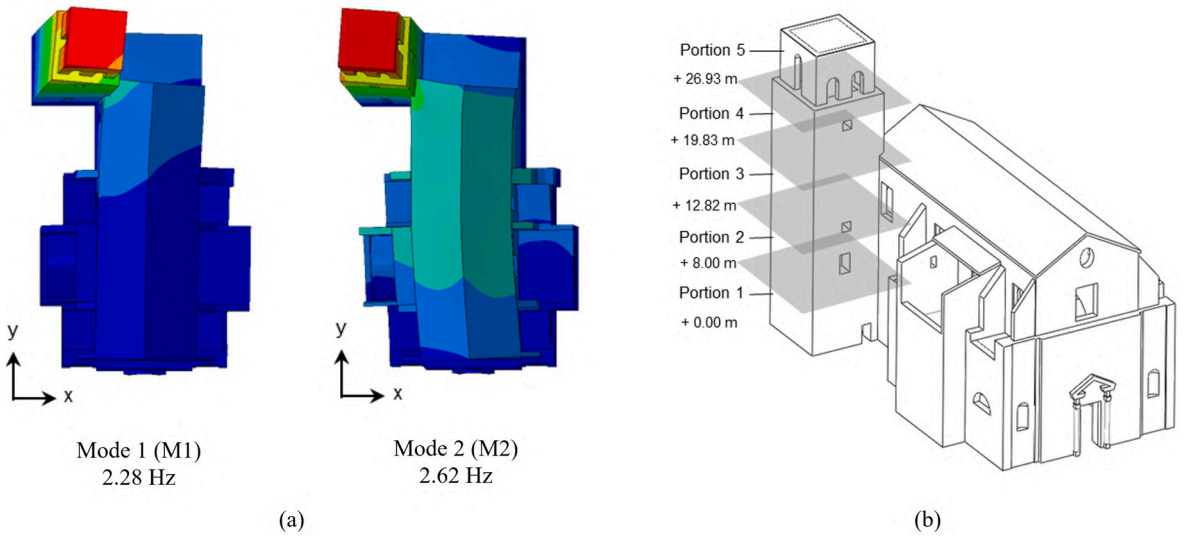

Fig. 9. San Francesco da Paola church: (a) first two natural modes of vibration, (b) division in portions of the bell tower for the application of the energy-based methodology.

5. Real case study application

In this section, the application of the energy-based methodology to the real case study of the bell tower of the San Francesco da Paola church is shown and discussed. It should be pointed out that the structural analyses here considered are not intended to be used for the structural seismic assessment of the church of San Francesco da Paola as a whole. Conversely, this monumental building is merely used as an application to assess the effectiveness of the energy-based methodology to detect the ultimate condition of the structure, when severe damage is observed without leading to softening in the pushover curve.

5.1. San Francesco da Paola church

The church of San Francesco da Paola ai Monti (Fig. 8) is located in the center of Rome. This religious building was built between 1624 and 1630 CE and completed in the early eighteenth century. The tower was built in the twelfth century, before the church, and a belfry was added to it only later. Made of brick masonry, it has a square base with a reinforcing spur and is pierced by slits, crowned in the 15th century with travertine corbels. The structure has a plan with a side of 8 m and a maximum height of 27m and was built with bricks of good workmanship in horizontal courses. The tower is characterized by the presence of few small openings. In [58], a detailed historical analysis of the San Francesco da Paola church is presented together with the ongoing damage mechanisms.

5.2. Numerical modelling

A 3D solid continuum finite element model of the structure has been developed accounting for both the bell tower and the adjacent church. Solid 4-node tetrahedral linear elements, with average dimension of 0.65m, have been adopted in the mesh, composed of 35,733 nodes and 142,884 elements.

Although the seismic analysis of churches is usually addressed through the decomposition in macro-elements [59,60,61], the adoption of a global model may reveal very useful for multiple aims, such as for supporting the definition of the macro-elements and address the choice, for each one, of the plausible mechanisms to be investigated, or defining the load redistribution among the macro-elements [62,63,64,65].

Moreover, the use of a global model is generally recommended to investigate the actual seismic behavior and, hence, to explicitly consider the mutual interactions between macro-elements [66], especially when an effective coupling among them is provided by rigid horizontal diaphragms, or in the presence of large interacting portions. Indeed, the seismic interaction may be crucial especially in the case of units with different architectural features leading to different dynamic properties, stiffness and strength [52].

A unique 3D solid continuum finite element model is considered, assuming continuity of material between the bell tower and the church (Fig. 9). It should be underlined that horizontal loads are applied in pushover analyses only on the bell tower unit, while the rest of the church is not loaded and simply used as constraint, and the base shear is computed on the overall structure, in the spirit of the methodology developed in [52], which has been successfully validated in an earthquake-damaged complex continuous masonry structure (medieval castle). In the framework of the application of the energy-based methodology, the same constitutive law and mechanical properties used in Section 4.1 are here adopted.

In order to obtain a preliminary insight on the dynamic behavior of the tower, a natural frequency analysis is performed on the 3D

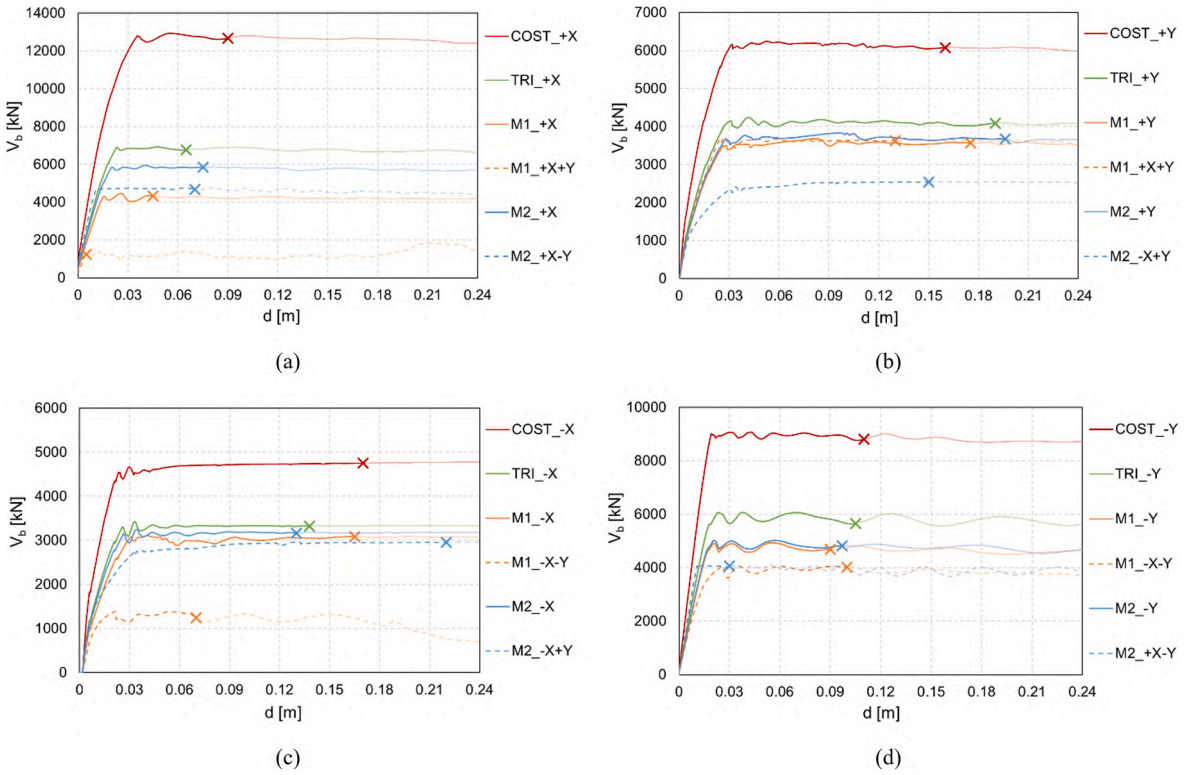

Fig. 10. Comparison of the pushover curves with different load patterns: (a) direction + x, (b) direction +y, (c) direction -x, (d) direction -y. A cross denotes the displacement at $\rho_{max} = 70\%$.

FE model. Fig. 9-a shows the deformed shapes of the first two natural modes of vibration, which are mainly first bending modes of the bell tower in two directions, characterized also by torsion due to the constrain offered by the church.

The results of the natural frequency analysis were used to define specific load patterns (LPs) to be applied to the bell tower. In particular, both modes M1 and M2 (Fig. 9-a) are characterized by displacement components along x and y (Fig. 9-a). The so-obtained LPs have been assumed to vary along × and y directions with a trapezoidal pattern and according to a cubic function in height. These LPs have been applied along one direction only (e.g., M1_+Y) or along both two directions (e.g., M1_+X + Y). Then, other LPs proportional to masses, with triangular (TRI) and constant (COST) shapes in height, have been also assumed in agreement with the Italian Code [3].

According to the preliminary analyses in Section 4, the bell tower is subdivided by means of horizontal planes into five portions (Fig. 9-b), in agreement with the specific architectural and construction peculiarities. Indeed, the top portion is represented by the belfry, while another section plane is at the height of the church. In addition, the height of the portions is comparable with the plan dimensions of the tower so it appears appropriate in order to apply the proposed energy-based methodology.

5.3. Numerical results

The results of the different simulations are compared in terms of pushover curves along the four directions (+x, -x, +y, -y, Fig. 10) and in terms of damage contour plots corresponding to the ultimate conditions (Fig. 11). The horizontal top displacement d is computed, analogously to the benchmarks, as the average of the horizontal displacement in the four nodes at the top corners of the tower (at the level below the belfry, i.e., at + 26.93 m, see Fig. 9-b).

It can be seen from the pushover curves (Fig. 10), no significant base shear degradation is observed (far from 20% decay, although significant horizontal top displacements are reached). Following the energy-based methodology introduced in Section 3, the diagram $d - \rho_i$ is evaluated for each i-th portion of the tower. Adopting the threshold obtained in the preliminary analyses, the displacement corresponding to $\rho_{max} = 70\%$ is selected (marked with a cross in Fig. 10), which is herein assumed to be the ultimate condition of the structure.

As it can be noted in Fig. 11, where tensile and compressive damage contour plots are shown at $\rho_{max} = 70\%$, significant through-thickness cracks can be observed in all cases (tensile damage), while crushing failures are not clearly observable. Basically, all the crack patterns shown in Fig. 11 highlight severe damage conditions in the structure. In light of these results, the damage patterns demonstrate the potential of the energy-based methodology to highlight ultimate conditions.

In addition, these results also put some light on the interaction effects between the tower and the church. By observing Fig. 11,

Fig. 11. Tensile and compressive damage maps at $\rho_{max} = 70\%$. Red and blue colors mean tensile and compressive damage, respectively. (For interpretation of the references to color in this figure legend, the reader is referred to the web version of this article.)

indeed, it is possible to compare the tensile damage contour plots obtained for the various LPs. Along the +y direction, the church acts as an asymmetrical constraint on the tower, and the cracks are very similar in all cases, i.e., they origin from the edge of the church and develop downward in a diagonal pattern. Pushing along the -y direction, the cracks are concentrated in the middle part of the tower,

while for M2_+X-Y, the +X component is preponderant and causes the cracks to quickly concentrate at the top part of the tower, as for the other analyses along that direction. In the -x direction, the various crack patterns show a detachment in the church-tower connection area, as well as diagonal cracks in the trunk of the tower. In conclusion, it emerges that the crack patterns are quite similar when considering COST, TRI, M1 and M2 distributions. Although this, large differences in terms of base shear are observed between the LPs (Fig. 10), especially for COST, which seems to significantly overestimate the capacity of the structure. Interestingly, LPs proportional to the natural modes show in all cases lower peak base shear values than TRI cases.

6. Conclusions

In this paper, an energy-based methodology has been introduced to estimate the ultimate condition of large-scale masonry structures. Such methodology appeared general and easy-to-use, and represents an alternative particularly useful when the strength degradation rule cannot be utilized (i.e., when the pushover curve does not show significant softening).

This methodology has been preliminary employed for tower-like masonry structures. Various simplified benchmarks subjected to several load scenarios have been utilized in pre-analyses to set the energy ratio thresholds. Then, the methodology has been tested on a real case study application, i.e., the bell tower of the San Francesco da Paola church in Rome, modelled through a suitable nonlinear continuum modelling approach.

Two main outcomes can be deduced by this case study application:

- the methodology is able to consistently identify ultimate conditions in the bell tower, characterized by severe damage levels even without significant softening in the pushover curve;
- LPs proportional to the natural modes (which consider the presence of the adjacent structure) show in all cases peak base shear values lower than TRI and COST LPs, although crack patterns are generally similar.

Further developments will concern the calibration and the application of the energy-based methodology to other typologies of complex continuous masonry structures.

Declaration of Competing Interest

The authors declare that they have no known competing financial interests or personal relationships that could have appeared to influence the work reported in this paper.

Data availability

Data will be made available on request.

Acknowledgements

This project has received funding from the European Union's Horizon 2020 re-search and innovation programme under the Marie Sklodowska-Curie grant agreement No 101029792 (HOLAHERIS project, "A holistic structural analysis method for cultural heritage structures conservation").

References

[1] EN 1998-3, Eurocode 8: design of structures for earthquake resistance-part 3: assessment and retrofitting of buildings. CEN (European Committee for Standardization), Brussels, Belgium, 2005.
[2] ASCE/SEI 41-17. Seismic evaluation and retrofit rehabilitation of existing buildings, 2014.
[3] NTC. Aggiornamento delle «Norme tecniche per le costruzioni». Gazzetta Ufficiale della Repubblica Italiana, 2018, Rome, Italy.
[4] CIRCOLARE, N. T. C. Circolare n. 7 del 21 Gennaio 2019, "Istruzioni per l'applicazione dell' «Aggiornamento delle "Norme tecniche per le costruzioni"» di cui al DM 17 gennaio 2018". CS LL. PP, 2019, Rome, Italy.
[5] "NewZealand Standard (NZS). 2004. Structural design actions- part 5: Earthquake actions. NZS 1170.5:2004, Wellington,New Zealand: Standard New Zealand".
[6] CNR-DT 212/2013. Guide for the probabilistic assessment of the seismic safety of the seismic safety of existing buildings. National Research Council of Italy, 2014.
[7] P. Fajfar, A nonlinear analysis method for performance-based seismic design, Earthq. Spectra 16 (3) (2000) 573–592.
[8] S. Lagomarsino, N. Abbas, C. Calderini, S. Cattari, R. Ginanni, R. Corradini, G. Marghella, F. Mattolin, V. Piovanello, Classification of cultural heritage assets and seismic damage variables for the identification of performance levels, in: Proceedings of 12th STREMAH conference, 5–7 September 2011, Chianciano Terme (Italy), 2011.
[9] S. Lagomarsino, S. Cattari, PERPETUATE guidelines for seismic performance-based assessment of cultural heritage masonry structures, Bull. Earthq. Eng. 13 (1) (2015) 13–47.
[10] DPCM 9/2/2011. Linee guida per la valutazione e la riduzione del rischio sismico del patrimonio culturale con riferimento alle Norme tecniche delle costruzioni di cui al decreto del Ministero delle Infrastrutture e dei trasporti del 14 gennaio, 2008.
[11] V. Sarhosis, G. Milani, A. Formisano, F. Fabbrocino, Evaluation of different approaches for the estimation of the seismic vulnerability of masonry towers, Bull. Earthq. Eng. 16 (2018) 1511–1545.
[12] M. Rossi, S. Cattari, S. Lagomarsino, Vulnerability assessment of Great Mosque of Algiers, Bull. Earthq. Eng. 13 (1) (2015) 369–388.
[13] S. Cattari, S. Degli Abbati, D. Ferretti, S. Lagomarsino, D. Ottonelli, M. Rossi, A. Tralli, The seismic behaviour of ancient masonry buildings after the earthquake in Emilia (Italy) on May 20th and 29th, Ingegneria Sismica 29 (2012) 87–119.
[14] M. Valente, G. Milani, Non-linear dynamic and static analyses on eight historical masonry towers in the North-East of Italy, Eng. Struct. 114 (2016) 241–270.

[15] A.M. D'Altri, V. Sarhosis, G. Milani, J. Rots, S. Cattari, S. Lagomarsino, S. de Miranda, Modeling strategies for the computational analysis of unreinforced masonry structures: review and classification, Arch. Comput. Meth. Eng. 27 (2020) 1153–1185.
[16] S. Cattari, B. Calderoni, I. Caliò, G. Camata, S. de Miranda, G. Magenes, G. Milani, A. Saetta, Nonlinear modeling of the seismic response of masonry structures: critical review and open issues towards engineering practice, Bull. Earthq. Eng. 20 (4) (2022) 1939–1997.
[17] P.B. Lourénço, R. De Borst, J.G. Rots, A plane stress softening plasticity model for orthotropic materials, Int. J. Numer. Meth. Eng. 40 (1997) 4033–4057.
[18] P.B. Lourenço, J.G. Rots, J. Blaauwendraad, Continuum model for masonry: parameter estimation and validation, J. Struct. Eng. 124 (6) (1998) 642–652.
[19] H.R. Lotfi, P.B. Shing, An appraisal of smeared crack models for masonry shear wall analysis, Comput. Struct. 41 (3) (1991) 413–425.
[20] L. Berto, A. Saetta, R. Scotta, R. Vitaliani, An orthotropic damage model for masonry structures, Int. J. Numer. Meth. Eng. 55 (2) (2002) 127–157.
[21] L. Pelà, M. Cervera, P. Roca, Continuum damage model for orthotropic materials: application to masonry, Comput. Methods Appl. Mech. Eng. 200 (9-12) (2011) 917–930.
[22] J. Toti, V. Gattulli, E. Sacco, Nonlocal damage propagation in the dynamics of masonry elements, Comput. Struct. 152 (2015) 215–227.
[23] A.M. D'Altri, G. Castellazzi, S. de Miranda, Collapse investigation of the Arquata del Tronto medieval fortress after the 2016 Central Italy seismic sequence, J. Build. Eng. 18 (2018) 245–251.
[24] G. Bartoli, B. Michele, V. Andrea, A numerical study on seismic risk assessment of historic masonry towers: a case study in San Gimignano, Bull. Earthq. Eng. 14 (2016) 1475–1518.
[25] G. Castellazzi, A.M. D'Altri, S. de Miranda, A. Chiozzi, A. Tralli, Numerical insights on the seismic behavior of a non-isolated historical masonry tower, Bull. Earthq. Eng. 16 (2) (2018) 933–961.
[26] M. Valente, G. Milani, Seismic assessment of historical masonry towers by means of simplified approaches and standard FEM, Constr. Build. Mater. 108 (2016) 74–104.
[27] F. Micelli, A. Cascardi, Structural assessment and seismic analysis of a 14th century masonry tower, Eng. Failure Anal. 107 (104198) (2020).
[28] M. Acito, M. Bocciarelli, C. Chesi, G. Milani, Collapse of the clock tower in Finale Emilia after the May 2012 Emilia Romagna earthquake sequence: Numerical insight, Eng. Struct. 72 (2014) 70–91.
[29] M. Betti, A. Vignoli, Numerical assessment of the static and seismic behaviour of the basilica of Santa Maria all'Impruneta (Italy), Constr. Build. Mater. 25 (2011) 4308–4324.
[30] G. Milani, M. Valente, Failure analysis of seven masonry churches severely damaged during the 2012 Emilia-Romagna (Italy) earthquake: non-linear dynamic analyses vs conventional static approaches, Eng. Fail. Anal. 54 (2015) 13–56.
[31] A. Elyamani, P. Roca, O. Caselles, J. Clapes, Seismic safety assessment of historical structures using updated numerical models: the case of Mallorca cathedral in Spain, Eng. Fail. Anal. 74 (2017) 54–79.
[32] G. Castellazzi, A.M. D'Altri, S. de Miranda, F. Ubertini, An innovative numerical modeling strategy for the structural analysis of historical monumental buildings, Eng. Struct. 132 (2017) 229–248.
[33] G. Milani, M. Valente, C. Alessandri, The narthex of the Church of the Nativity in Bethlehem: a non-linear finite element approach to predict the structural damage, Comput. Struct. 207 (2018) 3–18.
[34] L. Giresini, Energy-based method for identifying vulnerable macro-elements in historic masonry churches, Bull. Earthq. Eng. 14 (3) (2016) 919–942.
[35] M. Valente, Seismic vulnerability assessment and earthquake response of slender historical masonry bell towers in South-East Lombardia, Eng. Fail. Anal. 129 (2021) 105656.
[36] S. Cattari, M. Angiolilli, Multiscale procedure to assign structural damage levels in masonry buildings from observed or numerically simulated seismic performance, Bull. Earthq. Eng. 20 (13) (2022) 7561–7607.
[37] S. Marino, S. Cattari, S. Lagomarsino, Use of nonlinear static procedures for irregular URM buildings in literature and codes, in: Proceedings of 16th European Conference on Earthquake Engineering, Thessaloniki, Greece, 2018.
[38] A. Mouyiannou, M. Rota, A. Penna, G. Magenes, Identification of suitable limit states from nonlinear dynamic analyses of masonry structures, J. Earthq. Eng. 18 (2) (2014) 231–263.
[39] I. Iervolino, A. Spillatura, P. Bazzurro, Seismic reliability of code-conforming Italian buildings, J. Earthq. Eng. 22 (sup2) (2018) 5–27.
[40] I. Iervolino, R. Baraschino, A. Spillatura, Evolution of seismic reliability of code-conforming Italian buildings, J. Earthq. Eng. 27 (7) (2023) 1740–1768.
[41] S. Cattari, D. Camilletti, S. Lagomarsino, S. Bracchi, M. Rota, A. Penna, Masonry Italian code-conforming buildings. Part 2: nonlinear modelling and time-history analysis, J. Earthq. Eng. 22 (sup2) (2018) 2010–2040.
[42] A. Penna, M. Rota, S. Bracchi, M. Angiolilli, S. Cattari, S. Lagomarsino, Modelling and seismic response analysis of existing URM structures. Part 1: Archetypes of Italian modern buildings, J. Earthq. Eng. (2022) 1–27.
[43] S. Lagomarsino, A. Penna, A. Galasco, S. Cattari, TREMURI program: an equivalent frame model for the nonlinear seismic analysis of masonry buildings, Eng. Struct. 56 (2013) 1787–1799.
[44] G. Magenes, A method for pushover analysis in seismic assessment of masonry buildings, in: Proceedings of the12th World Conference on Earthquake Engineering, Auckland, New Zealand, 2000.
[45] P. Roca, C. Molins, A.R. Marí, Strength capacity of masonry wall structures by the equivalent frame method, J. Struct. Eng. 131 (2005) 1601–1610.
[46] S.Y. Chen, F.L. Moon, T. Yi, A macroelement for the nonlinear analysis of in-plane unreinforced masonry piers, Eng. Struct. 30 (2008) 2242–2252.
[47] G. Castellazzi, B. Pantò, G. Occhipinti, D. Talledo, L. Berto, G. Camata, A comparative study on a complex URM building: part II—issues on modelling and seismic analysis through continuum and discrete-macroelement models, Bull. Earthq. Eng. 20 (2022) 2159–2185.
[48] G. Occhipinti, I. Caliò, A.M. D'Altri, N. Grillanda, S. de Miranda, G. Milani, E. Spacone, Nonlinear finite and discrete element simulations of multi-storey masonry walls, Bull. Earthq. Eng. 20 (2022) 2219–2244.
[49] M. Acito, M. Buzzetti, C. Chesi, E. Magrinelli, G. Milani, Failures and damages of historical masonry structures induced by 2012 northern and 2016–17 Central Italy seismic sequences: critical issues and new perspectives towards seismic prevention, Eng. Fail. Anal. (2023), 107257.
[50] E. Coïsson, D. Ferretti, E. Lenticchia, Analysis of damage mechanisms suffered by Italian fortified buildings hit by earthquakes in the last 40 years, Bull. Earthq. Eng. 15 (2017) 5139–5166.
[51] S. Cattari, S. Degli Abbati, D. Ferretti, S. Lagomarsino, D. Ottonelli, A. Tralli, Damage assessment of fortresses after the 2012 Emilia earthquake (Italy), Bull. Earthq. Eng. 12 (2014) 2333–2365.
[52] S. Degli Abbati, A.M. D'Altri, D. Ottonelli, G. Castellazzi, S. Cattari, S. de Miranda, S. Lagomarsino, Seismic assessment of interacting structural units in complex historic masonry constructions by nonlinear static analyses, Comput. Struct. 213 (2019) 51–71.
[53] J. Lee, G.L. Fenves, Plastic-damage model for cyclic loading of concrete structures, J. Eng. Mech. 124 (8) (1998) 892–900.
[54] S. Cattari, D. Camilletti, A.M. D'Altri, S. Lagomarsino, On the use of continuum Finite Element and Equivalent Frame models for the seismic assessment of masonry walls, J. Build. Eng. 43 (2021), 102519.
[55] A.M. D'Altri, F. Cannizzaro, M. Petracca, D.A. Talledo, Nonlinear modelling of the seismic response of masonry structures: calibration strategies, Bull. Earthq. Eng. 20 (2022) 1999–2043.
[56] S. Petry, K. Beyer, Influence of boundary conditions and size effect on the drift capacity of URM, Eng. Struct. 65 (2014) 76–88.
[57] M. Bocciarelli, On the behavior factor of masonry towers, Soil Dyn. Earthq. Eng. 101 (2017) 81–89.
[58] P. Zimmaro, E. Ausilio, Geotechnical and structural investigation and monitoring techniques to determine the origin of ongoing damage processes in historical buildings: The Saint Francis of Paola Church in Rome case history, in: Geotechnical Engineering for the Preservation of Monuments and Historic Sites III, 2022.
[59] F. Doglioni, A. Moretti, V. Petrini, Le chiese e il terremoto. Dalla vulnerabilità constatata nel terremoto del Friuli al miglioramento antisismico nel restauro. Verso una politica di prevenzione, Lint Editoriale Associati, 1994.
[60] S. Lagomarsino, S. Podestà, Seismic vulnerability of ancient churches: I. Damage assessment and emergency planning, Earthq. Spectra 20 (2) (2004) 377–394.
[61] J. Leite, P.B. Lourenco, J.M. Ingham, Statistical assessment of damage to churches affected by the 2010–2011 Canterbury (New Zealand) earthquake sequence, J. Earthq. Eng. 17 (1) (2013) 73–97.

[62] M. Malena, A. Genoese, B. Panto', D. Spina, G. de Felice, Two steps procedure for the finite elements seismic analysis of the Casamari Gothic Church, Buildings 12 (9) (2022) 1451.
[63] S. Lagomarsino, D. Ottonelli, S. Cattari, Performance-based assessment of masonry churches: application to San Clemente Abbey in Castiglione a Casauria (Italy), in: Numerical Modeling of Masonry and Historical Structures, Woodhead Publishing, 2019, pp. 55–89.
[64] E. Mele, A. De Luca, A. Giordano, Modelling and analysis of a basilica under earthquake loading, J. Cult. Herit. 4 (4) (2003) 355–367.
[65] M. Valente, G. Brandonisio, G. Milani, A.D. Luca, Seismic response evaluation of ten tuff masonry churches with basilica plan through advanced numerical simulations, Int. J. Masonry Res. Innovation 5 (1) (2020) 1.
[66] M. Valente, Seismic behavior and damage assessment of two historical fortified masonry palaces with corner towers, Eng. Fail. Anal. 134 (2022), 106003.